REGULAR ARTICLE

blood advances

Comparison of antibody-based immunotherapeutics for malignant hematological disease in an experimental murine model

Karin Frebel,* Jörn C. Albring,* Anika Wohlgemuth, Christian Schwöppe, Stephan Hailfinger, Georg Lenz, and Matthias Stelljes

Department of Medicine A, Hematology, Oncology, Hemostaseology and Pneumology, University Hospital Münster, Münster, Germany

Key Points

- New mouse model allows for side-by-side comparison of antitumor activity and side effects of immunotherapeutics targeting the same epitope.
- Immunotherapies can be studied in a syngeneic or an allogeneic setting after stem cell transplant.

Antibody-based immunotherapies have revolutionized leukemia and lymphoma treatment, with animal studies being crucial in evaluating effectiveness and side effects. By targeting the evolutionary conserved Slamf7 immune receptor, which is naturally expressed by the murine multiple myeloma cell line MPC-11, we have developed a syngeneic mouse model for direct comparison of 3 immunotherapies: monoclonal antibodies (mAb), bispecific T-cell engagers (BiTE), and chimeric antigen receptor (CAR) T cells (CART), all targeting Slamf7. Slamf7-BiTE is a bispecific single-chain antibody consisting of α-Slamf7 and α-CD3 Fv fragments joined through a Gly-Ser linker, and Slamf7-CART comprises the α-Slamf7 Fv fragment fused to the msCD8α transmembrane and msCD28, 4-1BB, and CD3ζ intracellular signaling domains. Slamf7-BiTE and Slamf7-CART effectively killed MPC-11 cells in vitro, independently of Slamf7-mediated inhibitory signaling by self-ligation. After chimerizing the constant region of the rat–anti-mouse Slamf7 antibody to mouse Fc-immunoglobulin G2a for enhanced effector functions, Slamf7-mAb triggered antigen-specific antibody-dependent cellular cytotoxicity by binding to Fcγ receptor IV. In vivo, all 3 immunotherapies showed antitumor effects against Slamf7-expressing targets. Unlike Slamf7-mAb, Slamf7-BiTE led to considerable side effects in test animals, including weight loss and general malaise, which were also observed to a lesser extent after Slamf7-CART infusion. In allogeneic transplant, Slamf7-BiTE and Slamf7-CART maintained activity compared with the nontransplant setting, whereas Slamf7-mAb displayed enhanced antimyeloma activity. In summary, our model faithfully replicates treatment efficacy and side effects detected after human immunotherapy. It aids in developing and improving immunotherapies and may help devise novel approaches to mitigate undesired effects in steady state and allogeneic stem cell transplantation.

Introduction

Immunotherapy shows promise in treating hematological malignancies by harnessing the immune system's ability to target and kill cancer cells selectively. Unlike traditional chemotherapy and radiation therapy, which damage cells unspecifically, immunotherapies offer more targeted approaches. Various types of immunotherapies, such as monoclonal antibodies (mAb),[1] antibody-drug conjugates (ADCs),[2] bispecific T-cell engagers (BiTEs),[3] immune checkpoint inhibitors,[4] and chimeric antigen receptor

Submitted 11 September 2023; accepted 2 January 2024; prepublished online on *Blood Advances* First Edition 10 January 2024; final version published online 11 April 2024. https://doi.org/10.1182/bloodadvances.2023011647.

*K.F. and J.C.A. contributed equally to this study.

Original data and protocols available upon reasonable request from the corresponding author, Matthias Stelljes (stelljes@ukmuenster.de).

The full-text version of this article contains a data supplement.

(CAR) T cells (CART),[5] are currently used in clinical settings. However, response rates and side effects vary among patients,[6] necessitating further preclinical research to enhance their effectiveness and safety.

Animal models, particularly mouse models, are useful for studying the mechanisms of action and safety of immunotherapies.[7,8] Humanized mice with a functional human immune system provide a physiologically relevant environment for testing human-specific immunotherapies.[9,10] For example, humanized mice have been used to study the efficacy and toxicity of CD19-targeted CAR T-cell therapy for B-cell malignancies[11] and evaluate the effects of combination therapies on tumor growth and immune cell infiltration.[12] However, it is important to note that there are limitations to these models, including the variability in engraftment efficiency, immune cell development[13] and lineage skewing,[14] which can affect the reproducibility of results,[15] potential species-specific differences in immune function,[12,16] and the fact that these mice may not fully recapitulate the complexity and heterogeneity of the human immune system and the tumor microenvironment,[17] all of which can limit the translational potential of findings from humanized mouse studies.

Although syngeneic mouse models lack human-specific interactions and the ability to study the efficacy of human-specific immunotherapies, they have several advantages over humanized mouse models. They are less variable and have a more predictable immune response because their immune system, the tumor cells, and the host tissue are genetically identical, allowing for more relevant interactions between the immune system and the tumor microenvironment, which is critical for understanding the mechanisms of action of immunotherapies. Other advantages of syngeneic mouse models are that immunotherapies can be studied in fully immunocompetent hosts with physiologically intact immune responses, and they are more cost-effective and easier to maintain than humanized mouse models. In conclusion, both models complement each other and provide a more comprehensive understanding of immunotherapy's mechanisms of action and potential side effects, helping to develop more effective and safer treatments for cancer.

The signaling lymphocytic activation molecule family member 7 (Slamf7) is a cell surface glycoprotein that is primarily expressed on immune cells, including natural killer cells, plasma cells, and subsets of T cells. Due to its robust and high-level expression on malignant plasma cells,[18] SLAMF7 is a therapeutic target for the treatment of multiple myeloma.[19,20,21,22] We therefore selected murine Slamf7 (19A, CD319, CRACC, and CS1) as a model antigen for the direct comparison of several modalities of immunotherapy in a syngeneic mouse model of multiple myeloma. Furthermore, these therapeutic approaches could also be evaluated in the setting of allogeneic hematopoietic stem cell transplantation (aHSCT).

Methods

Antibody generation, production, and purification

Dark Agouti rats were immunized with recombinant mouse Slamf7 extracellular domain to generate a rat mAb against mouse Slamf7. Rapid amplification of complementary DNAs ends polymerase chain reaction identified the variable heavy and light sequences of positive hybridoma clones.[23,24] The resulting mAb was designated as Slamf7-mAb. A bispecific antibody against CD3ε and Slamf7, Slamf7-BiTE, was generated by cloning the single-chain variable fragment (scFv) of the anti-CD3ε antibody CRL-145 with a glycine-serine linker along with the previously identified scFv of the α-Slamf7 antibody.[25,26] Slamf7-BiTE constructs were produced in Freestyle CHO-S cells and purified.

Construction of murine stem cell virus retroviral vector encoding Slamf7-CART and transduction of mouse CD3$^+$ T cells

James Kochenderfer and Steven Rosenberg donated the CAR CD19 plasmid.[27] The Slamf7-CAR was created by combining the α-Slamf7 scFv with msCD8α's hinge and transmembrane domain, as well as intracellular signaling sequences from msCD28, 4-1BB, and CD3ζ.[28] This was cloned into the same murine stem cell virus retroviral vector used for CAR CD19. Mouse CD3$^+$ T cells were transduced following standard protocols.[29] Phoenix-Eco cells were transfected with DNA using FugeneHD, and transfection was confirmed the next day using pEGFP-N1 as a reporter. CD3/CD28-coated plates were used to activate CD3$^+$ T cells. RetroNectin-coated plates were used to transduce activated T cells with the retrovirus-containing supernatant from transfected Phoenix-Eco cells. The T cells were then cultured for 3 to 4 days in T-cell base medium supplemented with human interleukin (hIL)-7 and hIL-15. Fluorescence-activated cell sorting (FACS) analysis was used to detect CART$^+$ cells.

Mice and cell lines

BALB/c and CB6F1 hybrid mice obtained from Charles River (Sulzfeld, Germany) were housed in the Medical Faculty's animal facility in Muenster, Germany, under specific pathogen-free conditions. Female mice used for experiments were aged ~12 to 20 weeks, and those used for T cell isolation were aged around 4 to 8 weeks. The regional governmental authorities approved all procedures in accordance with European regulations. The BALB/c-derived plasmacytoma cell line MPC-11 (ATCC CCL-167)[30] was obtained from the American Type Culture Collection (Manassas, VA). MPC-11 wild type (wt) naturally expressed Slamf7, whereas the MPC-11 knockdown (kd) cell line expressed low levels of Slamf7 and was cultured under the same conditions as the wt cell line.

Generation of mouse Slamf7 kd using Crispr/Cas9

The Cas9-Puromycin vector (GenScript, L00693) was used to clone guide RNA primers that targeted Exon 2 and 3 of mouse Slamf7. MPC-11 cells were then transfected with the guide RNA primers using the FugeneHD transfection reagent (Promega, E2311) following the company's protocol. After transfection, the cells were selected using puromycin (invivoGen, ant-pr-1) for several weeks. Clones obtained from single-cell dilution that expressed Slamf7 at lower levels than MPC-11 wt were identified using flow cytometry (FACS) staining for Slamf7 expression.

Immune therapy

In the naive mouse model, IV injections were administered immediately after tumor inoculation. MAb treatment involved a dose of 10 mg per kg body weight (bw), whereas BiTE treatment comprised 1.25 mg per kg bw given twice a week. For CART treatment, mice received 100 mg per kg body weight cyclophosphamide for lymphodepleting chemotherapy intraperitoneally, followed by a single application of CART (10e6) on the next day, and

tumor injection 1 day later. Phosphate-buffered saline (PBS) injections served as controls. In the transplant setting, female CB6F1 (H-2Kbxd) mice received total body irradiation of 9 Gy 1 day before transplant. Bone marrow cells from donor female BALB/c (H-2 dissociation constant [Kd]) mice were administered via tail vein at 1e6/g bw. Tumor injection and immune therapy were initiated ~3 weeks after transplant.

Immunocytotoxicity/mouse FcyRIV activation

For in vitro cell cytotoxicity, MPC-11 wt and kd cell lines were labeled with BioTracker 488 Membrane Dye. Pan T cells were isolated from BALB/c spleens and mixed with tumor cells in a 10 to 1 effector-to-target ratio. The cell mixture was plated in a non-TC treated 96 U-well plate in assay medium. Antibodies were added to the cells at specific concentrations, and Slamf7-mAb was used to block T cells in some experiments. After 48 hours of incubation, cells were stained and analyzed using FACS.[31] Specific cytotoxicity was calculated based on live target cell counts, and T-cell activation was determined using CD69 expression. For antibody-dependent cellular cytotoxicity (ADCC) analysis, the mouse FcyRIV ADCC bioassay from Promega was used according to the manufacturer's protocol.

Results

Generation of 3 different functional antibody constructs targeting the relevant tumor antigen Slamf7

We initially generated novel rat mAb targeting Slamf7, resulting in the generation of 3 distinct clones (3.1.4, 49.1.1, and 12.3.1). Among these clones, clone 3.1.4, belonging to the immunoglobulin G2 (IgG2) isotype, was chosen for further investigations due to its superior binding affinity to Slamf7 compared with other clones (supplemental Figure 1). To study effector functions in murine models and to avoid cross-species reactivity, we chimerized the antibody by switching the invariable regions of the heavy and light chains of the rat Fc-IgG2a domain with murine Fc-IgG2a (Figure 1A,I). We confirmed the integrity of the purified antibody (Slamf7-mAb) by sodium dodecyl sulfate-polyacrylamide gel electrophoresis, which showed intact heavy (50 kDa) and light chains (25 kDa) compared with an isotype control (Figure 1B,I). Slamf7-mAb bound to Slamf7 endogenously expressed by the mouse myeloma cell line MPC-11 (MPC-11 wt), and no binding was observed after the Slamf7 gene had been knocked out[32] in MPC-11 cells (MPC-11 kd) using CRISPR-Cas9 (Figure 1C).

To generate a bispecific antibody against murine Slamf7 and murine CD3 (Slamf7-BiTE), we fused the scFv of the Slamf7 antibody (3.1.4) to the scFv of an antibody that recognizes the murine CD3ε chain (clone 145-2C11) using a glycine-serine linker (Figure 1D,I).[25] Purity of Slamf7-BiTE was confirmed by western blot using a carboxy terminus myc-tag (Figure 1E). Specific binding of Slamf7-BiTE was confirmed by staining of MPC-11 wt (Figure 1F, left) but not MPC-11 kd (Figure 1F, middle) and binding to $CD3^+$ T cells compared with isotype control (Figure 1F, right). The anti-CD3 scFv used in our constructs was derived from the 145-2C11 antibody, a hamster anti-mouse CD3ε antibody with relatively low affinity (Kd, ~7×10^{-8} M),[25,33,34,35] which has previously been used in functional BiTE constructs.[31] The efficacy and toxicities of antibody-based immunotherapies can be influenced by the individual binding affinities of the antigen-binding fragment. To address this, we conducted Biacore analyses of the Slamf7-mAb, resulting in a Kd of 6.97×10^{-10} M, and Slamf7-BiTE, with a slightly lower Kd of 6.64×10^{-9} M (supplemental Figure 2).

To obtain a CAR that specifically recognizes Slamf7, the variable regions of the hybridoma 3.1.4 light and heavy chains were cloned into a retroviral plasmid encoding the transmembrane domain of murine CD8α as well as the intracellular signaling sequences from murine CD28, 4-1BB, and CD3ζ (Figure 1G,I). We identified anti-Slamf7-CAR–transduced T cells (Slamf7-CART) by staining for scFv (Figure 1H). Transduction efficiencies varied between 25% and 40% (Figure 1H).

In vitro efficacy of BiTE antibody against Slamf7

To assess the cytotoxic effectiveness in vitro, we used MPC-11 wt cells that express Slamf7 (Figure 1C) as a target. At effector-to-target ratios ranging from 40:1 to 1:1, Slamf7-BiTE induced T cells to kill >80% of MPC-11 wt targets (Figure 2A, solid black). This effect was specific and required the expression of Slamf7 by target cells, because cell lysis was reduced to <40% and <4% at ratios of 40:1 and 1:1, respectively, when MPC-11 kd cells were used as targets (Figure 2A, dotted black). Therefore, Slamf7-BiTE increased the cytotoxicity of T cells by more than 20-fold at low effector-to-target ratios of 1:1, and even at very high ratios of 40:1, this increase remained higher than twofold and was statistically significant ($P = .007$). When an irrelevant BiTE was used, we observed very little T-cell–mediated cytotoxicity, which remained <13% regardless of whether the target cells expressed Slamf7 (Figure 2A, solid gray; Figure 2A, dotted gray). There was no statistically significant difference when Slamf7-BiTE–induced lysis of MPC-11 kd was compared with using an irrelevant BiTE and MPC-11 wt ($P = .1032$) or MPC-11 kd ($P = .1110$). At a constant 10:1 effector-to-target cell ratio, the Slamf7-BiTE–induced cytotoxicity of MPC-11 wt increased in a dose-dependent manner, showing a sigmoid slope with a half maximal target cell lysis (EC50) at a concentration of ~0.0247 μg/mL (Figure 2B, filled circles). No dose dependency was observed when MPC-11 kd targets (Figure 2B, filled squares) or irrelevant bispecific T-cell engager (irrBiTE) were used (Figure 2B, gray symbols), highlighting the requirement of Slamf7 expression by target cells for specific Slamf7-BiTE–mediated killing by T cells.

To exclude a relevant impact of Slamf7-mediated inhibitory signaling in Slamf7-BiTE–mediated activation, we blocked self-ligation of Slamf7 by preincubating effector T cells with an antibody directed against Slamf7 before measuring cytotoxicity (Figure 2C, solid gray). There was no significant difference ($P = .6995$) in cytotoxic activity at BiTE concentrations ranging from 0.021 to 15 μg/mL with (Figure 2C, solid gray) or without (Figure 2C, solid black) blocking of Slamf7 on T cells. As a control, incubation of T cells with monoclonal Slamf7 antibody alone did not result in any appreciable target cell lysis (Figure 2C, dotted gray).

To further assess the activation of T cells through the α-CD3 arm, the expression of CD69 was evaluated 48 hours after incubation with Slamf7-BiTE (Figure 2D, solid bars). Blocking Slamf7 on T cells (Figure 2D, solid gray) slightly increased CD69 expression

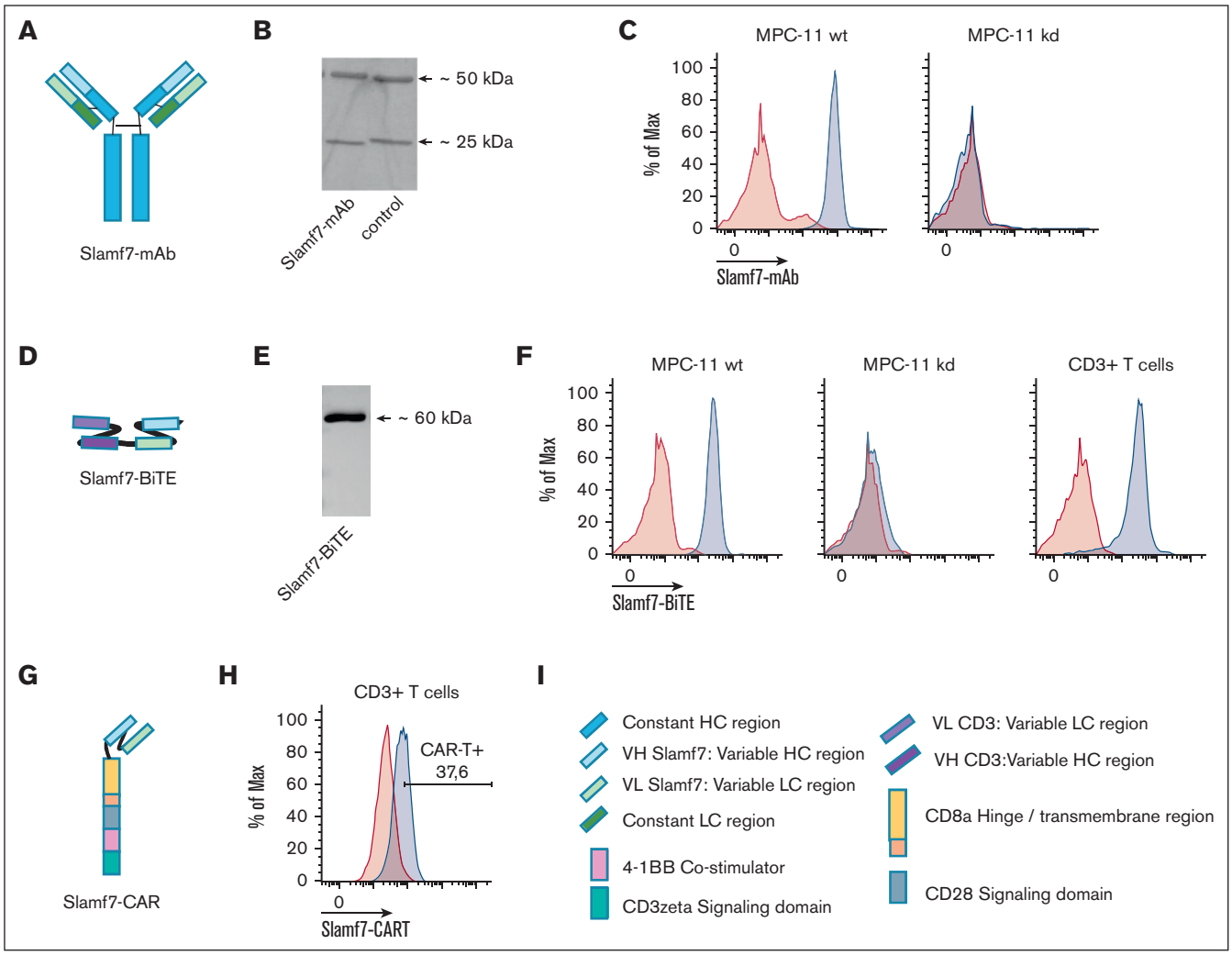

Figure 1. Structure and binding of Slamf7 immunotherapeutics. Shown is the molecular design of 3 different immunotherapeutic formats and binding to their specific targets. VH and VL sequences of original rat hybridoma clone 3-1-4 against Slamf7 (Biogenes) were cloned to generate the different types: (A) Schematic of chimeric Slamf7-mAb, a mAb containing mouse Fc–immunoglobulin G2a (Fc-IgG2a) and scFv of a-Slamf7. (B) Purity and integrity of antibody batches were controlled by sodium dodecyl sulfate-polyacrylamide gel electrophoresis showing intact heavy and light chains of Slamf7-mAb corresponding to correct sizes, isotype msIgG2a served as control. (C) Antibody binding to its target Slamf7 was analyzed by flow cytometry showing fluorescence signal in MPC-11 wt (blue profile), which is decreased when incubated with MPC-11 missing Slamf7 expression (MPC-11 kd), isotype control was used as negative control (red profile). (D) Schematic bispecific molecule with scFv parts of α-Slamf7 and α-msCD3 joined via flexible glycine-serine linker (Slamf7-BiTE). (E) Purified bispecific molecules were analyzed by western blot detecting myc-tag expressed on the carboxy terminus part of Slamf7- BiTE. (F) Flow cytometry analysis showed binding to msCD3 on T cells and to Slamf7 on MPC-11 wt ([red profile] isotype control; [blue profile] Slamf7-BiTE). (G) Schematic chimeric antigen T cell receptor was cloned containing sequences of CD8a hinge and transmembrane region, CD28-, 4-1BB–, and CD3ζ-signaling domain joined by scFv of Slamf7 (Slamf7-CAR). (H) After transduction of mouse T cells, they were labeled with an antibody detecting scFv Slamf7 on cell surfaces (blue), nontransduced T cells served as controls (red). An increase in fluorescence was assumed as signals for CART constructs. Usually transduction efficiency was around 25% to 40%. (I) Legend of domains. HC, heavy chain; kDa, kilodalton; LC, light chain; Ms, mouse; VH, variable heavy chain; VL, variable light chain.

levels compared with unblocked T cells (Figure 2D, solid black). This effect was small but statistically significant ($P = .037$) across a wide range of BiTE concentrations.

We used Jurkat cells with a luciferase reporter transgene that is activated upon binding of antibody to the murine FcγRIV receptor to evaluate the ability of Slamf7-mAb on ADCC. Slamf7-mAb induced luminescence beginning at concentrations of 0.016 μg/mL, reaching near maximal luminescence at 0.4 μg/mL, after which the signal reached a plateau at about 60 000 relative light units in the presence of MPC-11 wt target cells (Figure 2E, solid upright triangles). In the presence of MPC-11 kd luminescence remained <4500 relative light units even at the highest assessed antibody concentration of 10 μg/mL (Figure 2E, solid inverted triangles). No appreciable ADCC using luminescence as a surrogate parameter could be detected when an isotype control antibody (Figure 2E, circles) or Slamf7-BiTE (Figure 2E, squares) was incubated with MPC-11 wt or kd targets.

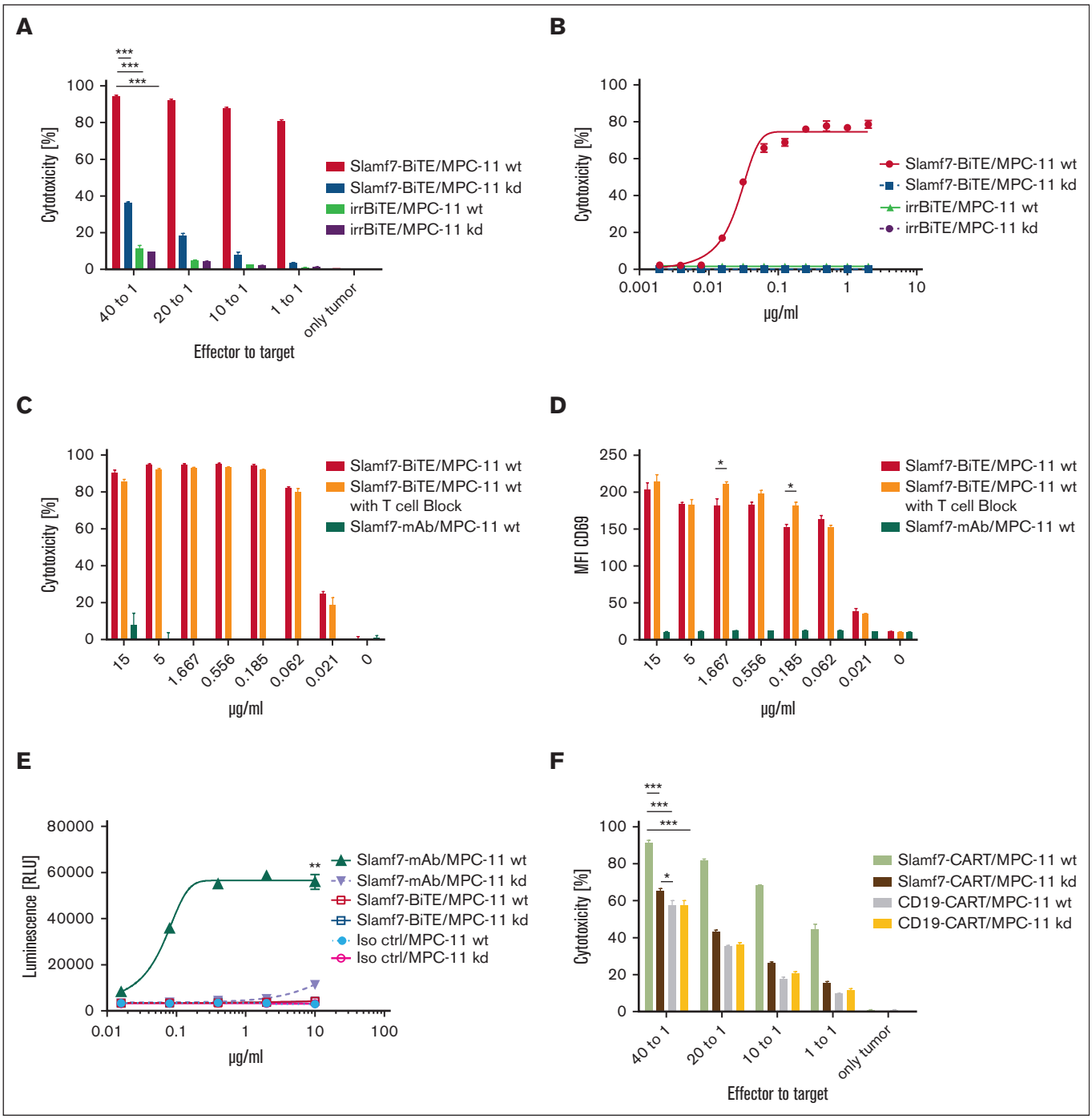

Figure 2. Mode of action of the different immunotherapeutic formats in vitro. (A) Slamf7-BiTE showed cytotoxic activity after 48 hours when incubated with unactivated mouse CD3$^+$ T cells and MPC-11 wt at different effector-to-target ratios at a constant concentration of 10 µg/mL. Compared with Slamf7-BiTE on MPC-11 kd cytotoxic activity is reduced but increases with amount of effector T cells. (B) Increasing concentration of Slamf7-BiTE on MPC-11 wt with constant effector-to-target ratio of 10 to 1 showed an increase of cytotoxic activity but not on MPC-11 kd, same for irrBiTE, a BiTE molecule with reduced binding to MPC-11 wt or kd. (C) The role of the self-ligand Slamf7 as a negative regulator of T-cell activation was analyzed in a cytotoxic assay in which effector T cells were preincubated with Slamf7-mAb. No difference in cytotoxic activity was noticed between blocked and unblocked T cells. Using Slamf7-mAb antibody instead of Slamf7-BiTE showed no activity. (D) Further T-cell activation was followed by the T-cell activation marker CD69 in flow cytometry analysis. Activation was reduced on a low level with unblocked T cells. (E) Using a Promega Bioassay for ADCC monoclonal Slamf7-mAb lead to an increase in luminescence correlating with activation of FcγRIV receptor on effector cells in presence of target tumor cell line MPC-11 wt, which is prevented by using isotype control or MPC-11 kd. (F) Mouse CD3$^+$ T cells transduced with CAR against Slamf7 (Salmf7-CART) showed significant cytotoxicity against MPC-11 wt after 24 hours, which is lowered when using MPC-11 kd or CD19-CART transduced cells. Data represent mean ± standard error of the mean (SEM) (n = 3). *$P \leq .05$; **$P < .01$; ***$P < .001$. Each assay was repeated at least twice.

To achieve sufficient transduction efficiencies of ~20% to 30%, freshly harvested T cells had to be activated using plate-bound antibodies directed against CD3 and CD28. Cytotoxicity of resulting Slamf7-CART was measured in a similar assay used to evaluate Slamf7-BiTE (Figure 2A). Slamf7-CART lysed ~45% of MPC-11 wt target cells at an effector-to-target ratios of 1:1 and >90% at 40:1 (Figure 2F, solid black bars). Cytotoxicity against Slamf7-expressing targets was significantly ($P < .01$) higher than that of MPC-11 kd cells expressing very little Slamf7 (Figure 2F, shaded black bars) or when irrelevant CAR T cells recognizing murine CD19, which is not expressed by MPC-11 cells (data not shown), were used (Figure 2F, solid and shaded black bars).

Effects of treatment with Slamf7-mAb vs Slamf7-BiTE vs Slamf7-CART in a naive syngeneic model

To compare the effects of different antibody-mediated immunotherapeutic formats on tumor regression in vivo, female BALB/c (H-2Kd) mice were challenged with the syngeneic BALB/c-derived myeloma cell line MPC-11 wt (H-2Kd) by injection into the right flank. Starting the same day mice received different doses of Slamf7-mAb and Slamf7-BiTE twice weekly (Figure 3A, bottom). For lymphodepletion before CART, mice received cyclophosphamide on day −2 and Slamf7-CART on day −1. Challenge with MPC-11 wt followed on day 0 as above (Figure 3A, top). In all experiments, tumor growth, bw, and general wellbeing of mice were assessed daily until experiments ended on day 14. Both, Slamf7-mAb and Slamf7-BiTE significantly reduced tumor growth compared with PBS control injections ($P < .5$). The observed inhibition of tumor growth was consistently more pronounced with Slamf7-BiTE than with Slamf7-mAb, although this difference was not statistically significant. (Figure 3B). Although Slamf7-mAb did not affect animal health and bw, Slamf7-BiTE caused significant bw loss of health. The undulating pattern of weight loss was correlated with individual injections of Slamf7-BiTE (Figure 3C). Typically, animals started to recover 24 hours after BiTE injection and regained their starting bw ~3 days later (Figure 3C).

Compared with control, Slamf7-CART led to retardation of tumor growth ($P > .1$). Even nontransduced T cells had some effect on tumor growth, but this was less pronounced (Figure 3D). Although all mice showed some degree of transient weight loss between days 1 and 5 after lymphodepletion, this was most evident in mice receiving Slamf7-CART (Figure 3E). CART cells expansion was documented by flow cytometry of the peripheral blood, in which $CD3^+$ T cells expressing scFv Slamf7 could readily be detected (Figure 3F).

Effects of treatment in a graft-versus-host disease model

Among hematological malignancies, relapse remains the primary cause of treatment failure after allogeneic transplantation.[36,37] To develop more effective therapeutic strategies for these patients, experimental models play a crucial role. In this study, we investigated the efficacy of different antibody-based immunotherapeutic formats in the context of aHSCT. For this purpose, we used a nonlethal parent-into-irradiated F1 model, which allows for continuous monitoring and intervention after transplantation.[38] In this model, very mild graft-versus-host disease results from partial major histocompatibility complex mismatch between H-2b haplotype donor cells and lethally irradiated H-2b/d haplotype recipients. Bone marrow from mice on the Balb/c background was transferred into lethally irradiated CB6F1 recipients on day 0 (Figure 4A, top left). Three weeks after transplant, mice received lymphodepleting chemotherapy, Slamf7-CART, and the tumor challenge on 3 consecutive days (Figure 4A, top right) or an injection with Slamf7-mAb or Slamf7-BiTE followed by tumor injection on the same day (Figure 4A, bottom right). In all experiments, tumor growth, bw, and general wellbeing of mice were assessed daily. To document engraftment and complete donor cell chimerism, we quantified the number of $H\text{-}2b^+$ and $H\text{-}2d^+$ cells in the peripheral blood by flow cytometry 2 weeks after aHSCT (Figure 4B). Successful transfer and expansion of Slamf7-CART was assessed at the end of each experiment by analyzing individual blood samples using flow cytometry and staining for CD3 and scFv Slamf7 (Figure 4C). The CAR of Slamf7-CART could only be detected in mice that received CAR T cells (Figure 4C, III). Treatment with Slamf7-mAb (Figure 4D, triangles) and Slamf7-BiTE (Figure 4D, filled squares) delayed tumor progression in this allogeneic transplantation model compared with PBS and irrBiTE control groups (Figure 4D, open squares and circles, respectively), as had been observed in the nontransplant setting (Figure 3B). Although animals that had received irrBiTE and Slamf7-mAb showed some degree of bw loss (Figure 4E, triangles and circles), the more pronounced and undulating weight loss in correlation to the administration of BiTE that we had observed before (Figure 3C) was only evident in mice that had been treated with Slamf7-BiTE (Figure 4E, filled squares). Unlike the animals in the nontransplant setting (Figure 3C,E), mice that had been treated with Slamf7-mAb, Slamf7-BiTE, or irrBiTE did not fully recover their bw by the end of the experiment (Figure 4E). No appreciable weight loss was detectable in control mice that had only received PBS injections (Figure 4E, open squares). Treatment of animals that had undergone aHSCT with Slamf7-CART significantly ($P = .152$) reduced tumor growth (Figure 4F, diamonds) and had no relevant impact on bw (Figure 4G), compared with control animals.

Discussion

Slamf7 is a self-associating member of the signaling lymphocytic activation molecule family that is evolutionary conserved across mammals and is expressed on cells of the immune system. Because of its high expression in multiple myeloma, it is a clinically relevant target in the treatment of patients with relapsed and refractory multiple myeloma. We have developed several immunotherapeutic approaches that use the identical complementarity-determining regions derived from a single mAb that recognizes murine Slamf7 (Figure 1). Using the myeloma cell line MPC-11 as a target, we performed comparative side-by-side analyses of a mAb, a BiTE, and CART under controlled experimental conditions in immunocompetent syngeneic hosts (Figures 2 and 3). In these model systems, antitumor effects could not only be studied in unmanipulated mice in the steady state (Figures 2 and 3) but also in mice that had previously received an allogeneic stem cell transplant (Figure 4). These results are meaningful because both, antitumor as well as side effects are modulated in a meaningful way after a stem cell transplant. Certain immunotherapies regularly cause detrimental side effects such as cytokine release syndrome (CRS) as well as immune effector cell-associated neurotoxicity syndrome that despite appropriate treatment can be life

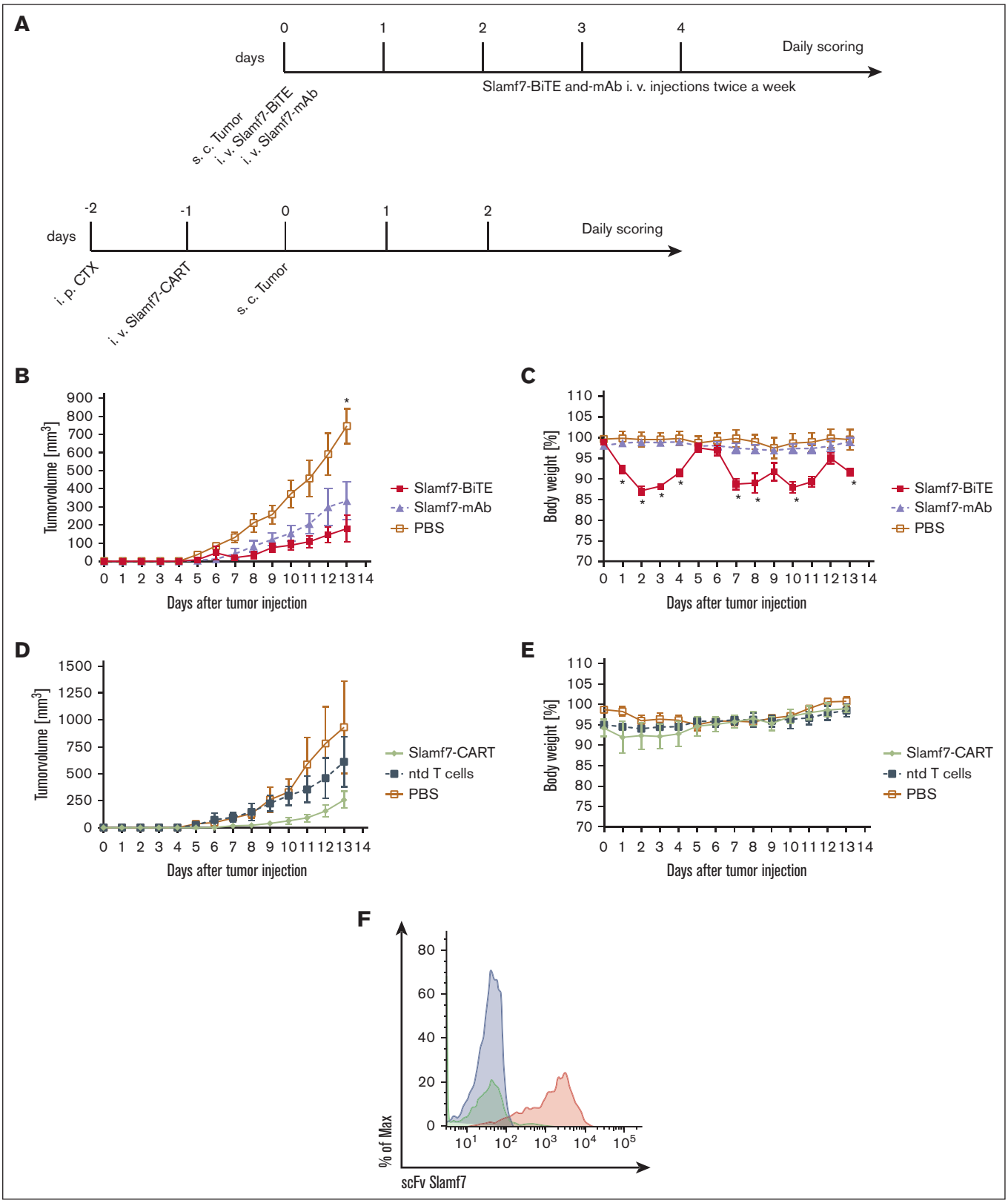

Figure 3. Immuntherapeutics targeting Slamf7 lead to reduced tumor growth in a naive syngeneic mouse model. (A) Schematic presentation of a syngeneic naive mouse model using female BALB/c mice as recipients, MPC-11 wt as tumor. Tumor injection was performed subcutaneously on the right flank, followed by intravenous Slamf7-BiTE (1.25 mg/kg bw per mouse) and Slamf7-mAb injection (10 mg/kg bw per mouse), this was defined as day 0. For CART experiments, cyclophosphamide was injected intraperitoneally 1 day before IV CART infusion (1e7 transduced T cells per mouse, ~20% transduction efficiency), followed next day by subcutaneous tumor injection. PBS

threatening in humans. Crucially, our models mimic these side effects by not only causing general malaise but also objective weight loss in test animals.

Previous studies have established that IV administration of the mAb 145-2C11, which was used in the construction of Slamf7-BiTE, can induce clinical and laboratory manifestations reminiscent of those observed in patients suffering from CRS. These manifestations include weight loss, hepatosplenomegaly, thrombocytopenia, increased vascular permeability, lung inflammation, and hypercytokinemia. Additionally, the investigation conducted in this regard involved the assessment of blood cytokine levels and gene expression in various tissues, such as lung, liver, and spleen, revealing significant upregulation of proinflammatory cytokines, including interleukin-2, interferon gamma, tumor necrosis factor-α, and interleukin-6, which preceded the onset of clinical CRS symptoms.[39] Although we have not independently confirmed these findings in this study, it is tempting to speculate that the strikingly similar symptoms observed after the administration of Slamf7-BiTE may also be indicative of CRS. Future studies using this model system should aim to address this hypothesis and further elucidate the underlying mechanisms.

SLAM receptors triggered by homotypic or heterotypic cell-cell interactions are modulating the activation and differentiation of a wide variety of immune cells, and Slamf7 has been identified as a negative regulator of T-cell activation.[40] Neither Slamf7-BiTE–mediated cytotoxicity nor the upregulation of the early T-cell activation marker CD69 after the engagement of the T-cell receptor by Slamf7-BiTE appeared to be affected significantly when we blocked self-ligation of Slamf7 by preincubating effector T cells with an antibody against Slamf7. This indicated that any inhibitory functions of Slamf7 had no relevant impact on cytotoxicity and T-cell activation in our model.

All therapeutic approaches showed significant antitumor activity in vitro as well as in vivo, but we did not observe complete tumor eradication under these experimental settings.

Although phenomena such as clonal exhaustion of effector T cells during chronic antigen exposure could contribute to this finding,[41] it is conceivable that reducing the number of injected cancer cells might mimic minimal residual disease better and hence allow for better tumor control or even eradication.[42,43] Further studies incorporating tumor heterogeneity and niche interactions are needed for a comprehensive minimal residual disease model. This study evaluated different antibody formats targeting the same antigen in a syngeneic model. We selected a representative format from chimeric mAbs, bispecific formats similar to blinatumomab, and CART constructs, all effective in mouse models.[28,31,44]

Clone 3.1.4 was selected for its intermediate affinity to Slamf7 to avoid off-target effects or rapid clearance. The BiTE construct used the CD3 arm (clone 145-2C11) for its specific recognition of mouse CD3ε and efficacy in T-cell activation. Amino terminus placement of the CD3 arm was chosen for superior T-cell activation.[25,31] The CART construct used a third-generation design, chosen for its effectiveness in preclinical mouse models, although not yet clinically approved.[28]

Although the 3 immunotherapeutic modalities chosen for this study constitute just a fraction of the available immunotherapeutic options, our model serves as a valuable instrument for enhancing the understanding and optimization of antitumor effects, particularly those influenced by structural variations. Moreover, the flexibility of our model allows for straightforward modifications to investigate and contrast other clinically pertinent constructs. This includes the exploration of second-generation CAR constructs with fewer signaling domains that have already been approved for clinical use.[45]

The study showed modest effects on tumor eradication, even in early stages, especially with established tumors (data not shown). Despite limitations, it lays a valuable foundation for future studies to explore various antigens, constructs, and tumor entities, expanding on the framework presented.

A subcutaneous tumor model was chosen for its reproducibility and quantifiable results, ideal for comparing 3 immunotherapies and assessing their effects on tumor growth and toxicity. However, this model does not fully replicate multiple myeloma, particularly the bone marrow niche crucial for immunotherapy.[46,47] Future research needs models that more accurately represent multiple myeloma and include preestablished tumor models to better understand the disease and treatment efficacy.[48] This will improve the evaluation of new therapies for multiple myeloma.

Although treatment options for patients with myeloma have improved significantly over the past decades, myeloma remains an incurable malignancy for the vast majority of patients.[49,50] Other targets besides SLAMF7 have been discovered, such as the B-cell maturation antigen (BCMA), which represents another promising target for treating myeloma. BCMA is highly expressed in multiple myeloma, and various immune therapeutics targeting BCMA have been developed, including the mAb-drug conjugate belantamab mafodotin as well as the BCMA-directed CART therapies, idecabtagene vicleucel and ciltacabtagene autoleucel, that have both been approved for multiple myeloma therapy. Although Slamf7 might not have the molecular prerequisites to be a suitable target for an ADC, our model system could be adapted by using a mAb as a basis that is more capable of internalizing ADC complexes.

Teclistamab is a recently approved bispecific antibody that targets the CD3 receptor and BCMA.[51] Similar to other T-cell–mediated therapeutics, ~72% of patients experience CRS after receiving teclistamab. Although preclinical studies using xenograft models inoculated with human myeloma and T cells demonstrated that

Figure 3 (continued) injections were used as control. Tumor size and bw were measured daily. (B) Both Slamf7-mAb (violet line) and Slamf7-BiTE (red line) lead to reduced tumor growth compared to PBS group (yellow line). (C) Slamf7-BiTE (red line) but not Slamf7-mAb (violet line) treatment had influence on bw. (D) Slamf7-CART animals (green line) showed reduced tumor growth compared to animals which received nontransduced T cells (nontransduced [ntd] T cells, blue line) or PBS (yellow line). (E) Treatment of animals with CART cells had no significant influence on bw in either group. (F) At the end of experiment successful engraftment of T cell transfer controlled using blood samples of animals of ntd T cells (green), PBS (blue) and Slamf7 CART (red) for flow cytometry analysis by detecting CD3+ cells expressing scFv Slamf7 of CART receptor on cell surface. Representative histograms are shown. Results for tumor growth and bw are representative of at least 2 independent experiments with n = 5 mice per group. The data are presented as mean ± SEM, $*P < .05$.

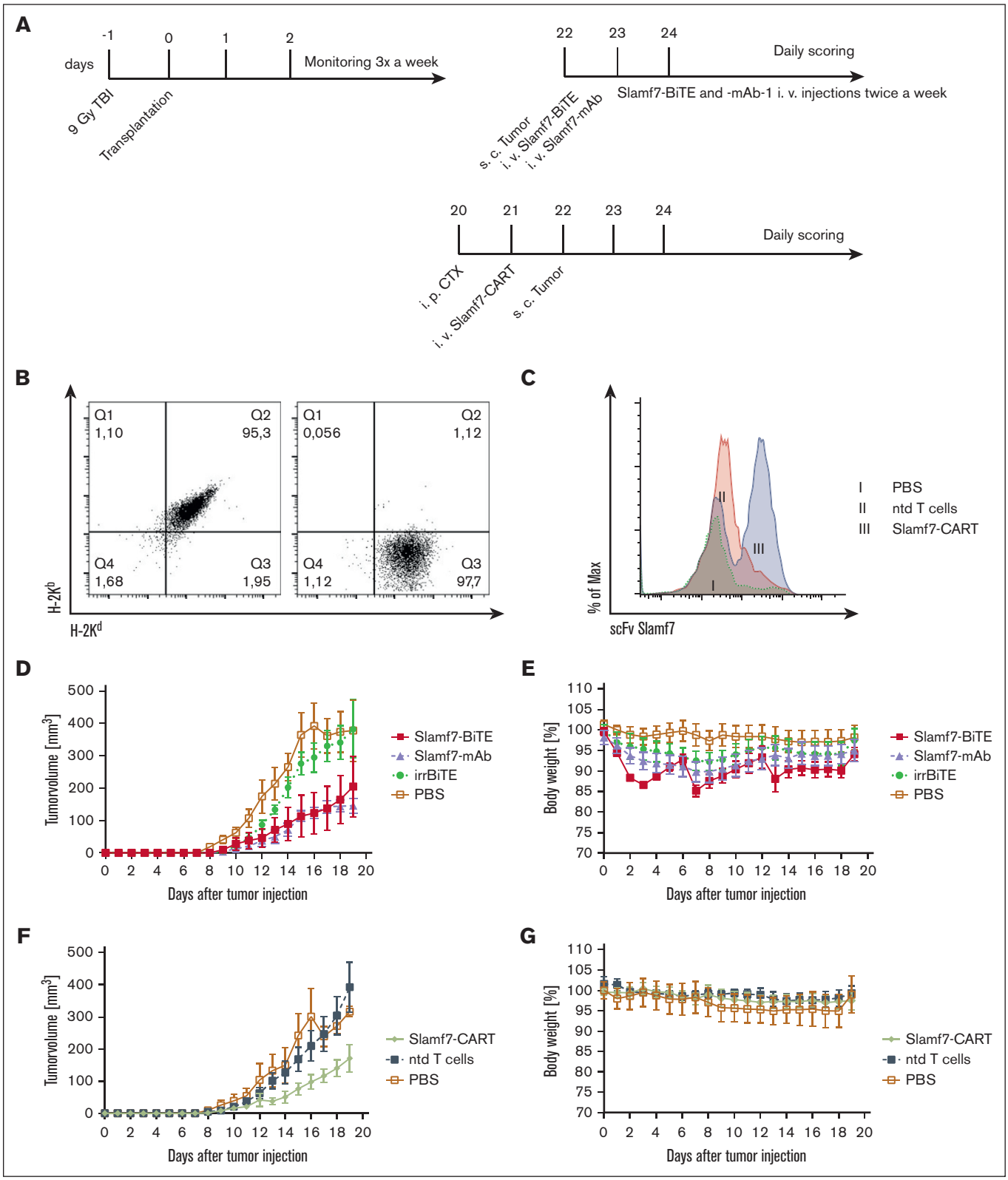

Figure 4. Immunotherapeutics targeting Slamf7 lead to reduced tumor growth in a parent-into-F1 model of stem cell transplant. (A) Schematic presentation in which female CB6F1 (H-2K^{bxd}) mice received total body irradiation (TBI) (9 Gy) 1 day before transplant of bone marrow of female BALB/c (H-2K^{d}). Three weeks after transplant, subcutaneous tumor injection of MPC-11 wt (H-2K^{d}) was performed on the right flank, followed by IV Slamf7-BiTE (1.25 mg/kg bw per mouse) and Slamf7-mAb injection (10 mg/kg bw per mouse) twice a week. Day of tumor injection was defined as day 0. For CART experiments, cyclophosphamide was injected intraperitoneally 1 day before IV CART

teclistamab had antitumor activity, they failed to flag adverse symptoms such as CRS.[52] Although relevant side effects can also be missed in syngeneic animals models as the infamous phase 1 study of the superagonistic anti-CD28 antibody TGN1412 has shown,[53] they can be useful in complementing efficacy data derived from xenograft models. The preserved interactions between immune cells and host tissues in syngeneic models provide valuable insights into the development of CRS, immune effector cell-associated neurotoxicity syndrome, or surrogate symptoms such as malaise or weight loss. These models play a crucial role in identifying potential adverse effects early in the drug development process and offer valuable opportunities to study and better understand undesired side effects.[54]

A preclinical in vivo model that is capable of assessing the impact of immune therapeutics on both tumor growth and potential adverse side effects resulting from the interactions between the treatment and the host's immune system is urgently required. Although current preclinical models, such as xenograft/humanized models, are effective at demonstrating efficacy against human tumor cells, they lack a functioning immune system and syngeneic host tissue, which fails to accurately reflect the complex interactions between the treatment and the host organism. Our newly developed model of hematological disease allows for side-by-side comparisons of different immunotherapies while using a syngeneic and functioning immune system. Furthermore, our model accurately recapitulates the desired antitumor activity of individual agents as well as adverse effects regularly observed with these therapies, such as CRS and neurotoxicity. These attributes will allow for further studies to better understand how desired antitumor activity and detrimental side effects are intertwined at the cellular and molecular level. Therefore, although more research is warranted to corroborate the link between clinical symptoms and CRS as well as to test the activity of immunotherapies against other tumor entities and antigens, our model represents a valuable basis for preclinical tools that can be adapted for the development and study of a wide variety of immunotherapeutic treatment modalities.

Authorship

Contribution: K.F., J.C.A., and M.S. designed the study; K.F., A.W., and C.S. performed the key experiments; and K.F., J.C.A., A.W., C.S., S.H., G.L., and M.S. interpreted the data and wrote and rewieved the manuscript.

Conflict-of-interest disclosure: The authors declare no competing financial interests.

ORCID profiles: J.C.A., 0000-0002-5534-7250; M.S., 0000-0002-9331-5145.

Correspondence: Matthias Stelljes, Department of Medicine A, Hematology, Oncology, and Pneumology, University Hospital Münster, Albert-Schweitzer-Campus 1, 48149 Münster, Germany; email: stelljes@ukmuenster.de.

References

1. Weiner LM, Surana R, Wang S. Monoclonal antibodies: versatile platforms for cancer immunotherapy. *Nat Rev Immunol*. 2010;10(5):317-327.
2. Lambert JM, Berkenblit A. Antibody-drug conjugates for cancer treatment. *Annu Rev Med*. 2018;69:191-207.
3. Bargou R, Leo E, Zugmaier G, et al. Tumor regression in cancer patients by very low doses of a T cell-engaging antibody. *Science*. 2008;321(5891):974-977.
4. Sharma P, Allison JP. The future of immune checkpoint therapy. *Science*. 2015;348(6230):56-61.
5. June CH, O'Connor RS, Kawalekar OU, Ghassemi S, Milone MC. CAR T cell immunotherapy for human cancer. *Science*. 2018;359(6382):1361-1365.
6. Sharma P, Allison JP. Immune checkpoint targeting in cancer therapy: toward combination strategies with curative potential. *Cell*. 2015;161(2):205-214.
7. Chesi M, Matthews GM, Garbitt VM, et al. Drug response in a genetically engineered mouse model of multiple myeloma is predictive of clinical efficacy. *Blood*. 2012;120(2):376-385.
8. Pardoll DM. The blockade of immune checkpoints in cancer immunotherapy. *Nat Rev Cancer*. 2012;12(4):252-264.
9. Allen TM, Brehm MA, Bridges S, et al. Humanized immune system mouse models: progress, challenges and opportunities. *Nat Immunol*. 2019;20(7):770-774.
10. Rongvaux A, Willinger T, Takizawa H, et al. Human thrombopoietin knockin mice efficiently support human hematopoiesis in vivo. *Proc Natl Acad Sci U S A*. 2011;108(6):2378-2383.

Figure 4 (continued) infusion (1e7 transduced T cells per mouse, ~20% transduction efficiency), followed next day by subcutaneous tumor injection. Tumor size and bw were measured daily. (B) Successful bone marrow engraftment was controlled using blood samples from animals that received transplant for flow cytometry analysis staining with H-2K^b (C57BL/6) and H-2K^d (BALB/c), showing just a signal for H-2K^d expression in the transplanted animals (right dot plot). Animals that did not receive transplant showed expression for both major histocompatibility complex-class I markers (left dot plot). (C) At the end of experiment, engraftment of CART cells was controlled using blood samples of animals from every group. Flow cytometry analysis showed CD3$^+$ T cells expressing scFv Slamf7-1 of CART receptor on cell surface only in Slamf7-CART group. Representative histograms from 1 animal of each group are shown. (D) Treatment of CB6F1 mice that received transplant with Slamf7-mAb (violet triangle) and Slamf7-BiTE (red rectangle) showed reduced tumor growth compared with group receiving PBS or irrBiTE as control (orange rectangle/green circle). (E) Slamf7-BiTE, Slamf7-mAb and irrBiTE treatment has an impact on bw compared with PBS group, whereas Slamf7-BiTE had the strongest. (F) CB6F1 mice treated with Slamf7-CART cells (green line) had smaller tumors as in control groups (ntd T cells, PBS). (G) bw was not influenced by treatment with Slamf7-CART cells. Representative FACS profiles are shown. Results for tumor growth and bw are representative of 5 mice per group. The data represented as mean ± SEM, $P < .05$.

11. Jin CH, Xia J, Rafiq S, et al. Modeling anti-CD19 CAR T cell therapy in humanized mice with human immunity and autologous leukemia. *EBioMedicine*. 2019;39:173-181.
12. Rongvaux A, Willinger T, Martinek J, et al. Development and function of human innate immune cells in a humanized mouse model [published correction appears in *Nat Biotechnol*. 2017;35(12):1211]. *Nat Biotechnol*. 2014;32(4):364-372.
13. Pearson T, Greiner DL, Shultz LD. Creation of "humanized" mice to study human immunity. *Curr Protoc Immunol*. 2008;Chapter 15:15.21.1-15.21.21.
14. Billerbeck E, Barry WT, Mu K, Dorner M, Rice CM, Ploss A. Development of human CD4+FoxP3+ regulatory T cells in human stem cell factor-granulocyte-macrophage colony-stimulating factor-and interleukin-3-expressing NOD-SCID IL2Rγ(null) humanized mice. *Blood*. 2011;117(11):3076-3086.
15. Brehm MA, Wiles MV, Greiner DL, Shultz LD. Generation of improved humanized mouse models for human infectious diseases. *J Immunol Methods*. 2014;410:3-17.
16. Mestas J, Hughes CC. Of mice and not men: differences between mouse and human immunology. *J Immunol*. 2004;172(5):2731-2738.
17. Walsh NC, Kenney LL, Jangalwe S, et al. Humanized mouse models of clinical disease. *Annu Rev Pathol*. 2017;12:187-215.
18. Frigyesi I, Adolfsson J, Ali M, et al. Robust isolation of malignant plasma cells in multiple myeloma. *Blood*. 2014;123(9):1336-1340.
19. Dimopoulos MA, Dytfeld D, Grosicki S, et al. Elotuzumab plus pomalidomide and dexamethasone for multiple myeloma. *N Engl J Med*. 2018;379(19):1811-1822.
20. Hsi ED, Steinle R, Balasa B, et al. CS1, a potential new therapeutic antibody target for the treatment of multiple myeloma. *Clin Cancer Res*. 2008;14(9):2775-2784.
21. Collins SM, Bakan CE, Swartzel GD, et al. Elotuzumab directly enhances NK cell cytotoxicity against myeloma via CS1 ligation: evidence for augmented NK cell function complementing ADCC. *Cancer Immunol Immunother*. 2013;62(12):1841-1849.
22. Kurdi AT, Glavey SV, Bezman NA, et al. Antibody-dependent cellular phagocytosis by macrophages is a novel mechanism of action of elotuzumab. *Mol Cancer Ther*. 2018;17(7):1454-1463.
23. Zhang Y, Frohman MA. Cloning cDNA ends using RACE. *Methods Mol Med*. 1998;13:81-105.
24. Bradbury A. Cloning hybridoma cDNA by RACE. In: Kontermann R, Dübel S, eds. *Antibody Engineering*. Vol. 1. Springer-Verlag Berlin Heidelberg; 2010:56-61.
25. Leo O, Foo M, Sachs DH, Samelson LE, Bluestone JA. Identification of a monoclonal antibody specific for a murine T3 polypeptide. *Proc Natl Acad Sci U S A*. 1987;84(5):1374-1378.
26. Mack M, Riethmüller G, Kufer P. A small bispecific antibody construct expressed as a functional single-chain molecule with high tumor cell cytotoxicity. *Proc Natl Acad Sci U S A*. 1995;92(15):7021-7025.
27. Kochenderfer JN, Yu Z, Frasheri D, Restifo NP, Rosenberg SA. Adoptive transfer of syngeneic T cells transduced with a chimeric antigen receptor that recognizes murine CD19 can eradicate lymphoma and normal B cells. *Blood*. 2010;116(19):3875-3886.
28. Chinnasamy D, Yu Z, Theoret MR, et al. Gene therapy using genetically modified lymphocytes targeting VEGFR-2 inhibits the growth of vascularized syngenic tumors in mice. *J Clin Invest*. 2010;120(11):3953-3968.
29. Lanitis E, Rota G, Kosti P, et al. Optimized gene engineering of murine CAR-T cells reveals the beneficial effects of IL-15 coexpression. *J Exp Med*. 2021;218(2):e20192203.
30. Coffino P, Laskov R, Scharff MD. Immunoglobulin production: method for quantitatively detecting variant myeloma cells. *Science*. 1970;167(3915):186-188.
31. Schlereth B, Kleindienst P, Fichtner I, et al. Potent inhibition of local and disseminated tumor growth in immunocompetent mouse models by a bispecific antibody construct specific for Murine CD3. *Cancer Immunol Immunother*. 2006;55(7):785-796.
32. Ishibashi A, Saga K, Hisatomi Y, Li Y, Kaneda Y, Nimura K. A simple method using CRISPR-Cas9 to knock-out genes in murine cancerous cell lines. *Sci Rep*. 2020;10(1):22345.
33. Alegre ML, Tso JY, Sattar HA, et al. An anti-murine CD3 monoclonal antibody with a low affinity for Fc gamma receptors suppresses transplantation responses while minimizing acute toxicity and immunogenicity. *J Immunol*. 1995;155(3):1544-1555.
34. Jost CR, Titus JA, Kurucz I, Segal DM. A single-chain bispecific Fv2 molecule produced in mammalian cells redirects lysis by activated CTL. *Mol Immunol*. 1996;33(2):211-219.
35. Chen BM, Al-Aghbar MA, Lee CH, et al. The affinity of elongated membrane-tethered ligands determines potency of T cell receptor triggering. *Front Immunol*. 2017;8:793.
36. Horowitz M, Schreiber H, Elder A, et al. Epidemiology and biology of relapse after stem cell transplantation. *Bone Marrow Transplant*. 2018;53(11):1379-1389.
37. Zeiser R, Vago L. Mechanisms of immune escape after allogeneic hematopoietic cell transplantation. *Blood*. 2019;133(12):1290-1297.
38. Stelljes M, Strothotte R, Pauels HG, et al. Graft-versus-host disease after allogeneic hematopoietic stem cell transplantation induces a CD8+ T cell-mediated graft-versus-tumor effect that is independent of the recognition of alloantigenic tumor targets. *Blood*. 2004;104(4):1210-1216.
39. Nouveau L, Buatois V, Cons L, et al. Immunological analysis of the murine anti-CD3-induced cytokine release syndrome model and therapeutic efficacy of anti-cytokine antibodies. *Eur J Immunol*. 2021;51(8):2074-2085.

40. Cruz-Munoz ME, Dong Z, Shi X, Zhang S, Veillette A. Influence of CRACC, a SLAM family receptor coupled to the adaptor EAT-2, on natural killer cell function. *Nat Immunol*. 2009;10(3):297-305.
41. Daniel B, Yost KE, Hsiung S, et al. Divergent clonal differentiation trajectories of T cell exhaustion. *Nat Immunol*. 2022;23(11):1614-1627.
42. Albring JC, Sandau MM, Rapaport AS, et al. Targeting of B and T lymphocyte associated (BTLA) prevents graft-versus-host disease without global immunosuppression. *J Exp Med*. 2010;207(12):2551-2559.
43. Edinger M, Cao YA, Verneris MR, Bachmann MH, Contag CH, Negrin RS. Revealing lymphoma growth and the efficacy of immune cell therapies using in vivo bioluminescence imaging. *Blood*. 2003;101(2):640-648.
44. Nagorsen D, Bargou R, Ruttinger D, Kufer P, Baeuerle PA, Zugmaier G. Immunotherapy of lymphoma and leukemia with T-cell engaging BiTE antibody blinatumomab. *Leuk Lymphoma*. 2009;50(6):886-891.
45. Cappell KM, Kochenderfer JN. A comparison of chimeric antigen receptors containing CD28 versus 4-1BB costimulatory domains. *Nat Rev Clin Oncol*. 2021;18(11):715-727.
46. Ghobrial IM, Detappe A, Anderson KC, Steensma DP. The bone-marrow niche in MDS and MGUS: implications for AML and MM. *Nat Rev Clin Oncol*. 2018;15(4):219-233.
47. García-Ortiz A, Rodríguez-García Y, Encinas J, et al. The role of tumor microenvironment in multiple myeloma development and progression. *Cancers (Basel)*. 2021;13(2):217.
48. Mehdi SH, Nafees S, Mehdi SJ, Morris CA, Mashouri L, Yoon D. Animal models of multiple myeloma bone disease. *Front Genet*. 2021;12:640954.
49. Greil C, Engelhardt M, Ihorst G, et al. Allogeneic transplantation of multiple myeloma patients may allow long-term survival in carefully selected patients with acceptable toxicity and preserved quality of life. *Haematologica*. 2019;104(2):370-379.
50. Greil C, Engelhardt M, Finke J, Wäsch R. Allogeneic stem cell transplantation in multiple myeloma. *Cancers (Basel)*. 2021;14(1):55.
51. Moreau P, Garfall AL, van de Donk NWCJ, et al. Teclistamab in relapsed or refractory multiple myeloma. *N Engl J Med*. 2022;387(6):495-505.
52. Pillarisetti K, Powers G, Luistro L, et al. Teclistamab is an active T cell-redirecting bispecific antibody against B-cell maturation antigen for multiple myeloma. *Blood Adv*. 2020;4(18):4538-4549.
53. St Clair EW. The calm after the cytokine storm: lessons from the TGN1412 trial [published correction appears in *J Clin Invest*. 2008;118(6):2365. *J Clin Invest*. 2008;118(6):1344-1347.
54. Parker KR, Migliorini D, Perkey E, et al. Single-cell analyses identify brain mural cells expressing CD19 as potential off-tumor targets for CAR-T immunotherapies. *Cell*. 2020;183(1):126-142.e17.